

Article

Network Coordination between High-Voltage DC and High-Voltage AC Transmission Systems Using Flexible AC Transmission System Controllers

Nomihla Wandile Ndlela * and Innocent Ewean Davidson 

Department of Electrical Power Engineering, Durban University of Technology, Durban 4000, South Africa

* Correspondence: 21312861@dut4life.ac.za

Abstract: The strategic intent of the African Union is to develop a “Smart Integrated African Electric Power Super Grid” driven by modern tools and advances in high-voltage direct current (HVDC) engineering and flexible alternating current technology systems (FACTS), which is central in supporting Africa’s sustained economic growth and development. The southern African region, including South Africa, is beset by the critical challenges of perennial load-shedding, which impedes economic growth and aggravates unemployment. This has led to the insecurity of electricity supplies and degraded the quality of life. The parallel operation of high-voltage direct current (HVDC) and flexible AC technology systems (FACTS) controllers is gaining traction as system conditions become more complex, such as weak power networks which requires increased stability requirements, resulting in load-shedding and power outages. These adversely affect business productivity and adversely affect GDP and economic growth. Thus, the application of innovative technologies such as HVDC links can stabilize weak power systems. It is established that HVDC delivery systems reduce losses in long transmission lines transporting bulk power compared with high-voltage alternating current (HVAC) transmission lines for power wheeling. This paper evaluates the parallel operation of the Cahora Bassa 1414 km bipolar HVDC link and a weak parallel 400/330 kV alternating current (AC) link. It demonstrates the use of FACTS controllers to enhance the technical performance of an existing network, such as voltage control, and technical loss reduction. It combines an HVDC line commutated converter (LCC) and HVAC transmission lines, in hybrid notation to increase the voltage stability of the system by controlling the reactive power with a Static Var Compensator (SVC). These modern tools can increase the transmission power controllability and stability of the power network. In this study, HVDC–LCC was used with a setpoint of 1000 MW in conjunction with the 850 MVar SVC. The results show that the technical losses were reduced by 0.24% from 84.32 MW to 60.32 MW as Apollo 275 kV SVC was utilized for voltage control. The network analysis was performed using DIGSILENT PowerFactory software that is manufactured by DIGSILENT GmbH at Gomaringen, Germany



Citation: Ndlela, N.W.; Davidson, I.E. Network Coordination between High-Voltage DC and High-Voltage AC Transmission Systems Using Flexible AC Transmission System Controllers. *Energies* **2022**, *15*, 7402. <https://doi.org/10.3390/en15197402>

Academic Editors: Mazaher Karimi, Abu-Siada Ahmed and Andrea Mariscotti

Received: 18 July 2022

Accepted: 5 October 2022

Published: 9 October 2022

Publisher’s Note: MDPI stays neutral with regard to jurisdictional claims in published maps and institutional affiliations.

Keywords: power interconnections; power exchange; HVDC–LCC; Static Var Compensator; Songo–Apollo HVDC line



Copyright: © 2022 by the authors. Licensee MDPI, Basel, Switzerland. This article is an open access article distributed under the terms and conditions of the Creative Commons Attribution (CC BY) license (<https://creativecommons.org/licenses/by/4.0/>).

1. Introduction

Modern power systems are extremely complex and they are required to meet the increasing demand for electricity with acceptable quality and pricing [1]. This study evaluated the application of power-electronics-based FACTS controllers in electric power systems [2], with reference to the Cahora Bassa bi-polar HVDC link between Mozambique and South Africa. Hingorani [2] pioneered the concept of FACTS in 1988 by using power electronics controllers to increase power transfer in existing AC transmission lines, voltage management, and system stability without adding additional lines [1]. In Africa, the first power exchange was between the Democratic Republic of the Congo (DRC), Zambia, and Zimbabwe, and was built in 1960 [3]. By 1970, an interconnection was established between

Mozambique and South Africa, and between Botswana and South Africa in 1995 followed by a 400 kV link established between Zimbabwe and South Africa. Presently, only Tanzania, Angola, and Malawi do not have any interconnections with other countries; however, new links are planned [4]. In Africa, the first VSC-based (voltage source converter), the Caprivi HVDC interconnector between Namibia and Zambia, was commissioned in 2010 as shown in Figure 1 [5]. The overhead line is 950 km long and operates at 350 kV DC [6]. It has been proposed to use highly complex power system controllers to integrate African national power grids into one super-grid that can accept a large penetration of renewable powers, without compromising power quality, active and reactive power flow, and voltage and power system stability [7,8]. The proposed super-grid will be constructed using HVDC and flexible AC transmission systems along with dedicated AC/DC interconnectors and smart grids. DC interconnectors will be used to segment the entire continent's power systems into four or five large asynchronous segments (regions). Asynchronous segments will prevent AC fault propagation between segments while allowing power exchange between different parts of the super-grid, with minimum difficulty for grid code unification or the harmonization of regulatory regimes across the continent as each segment maintains its autonomy [7]. The Caprivi Link can be extended to a multi-terminal DC (MT-HVDC) system as part of the African super-grid, capable of harnessing gigawatts of hydro-power from the Congo River to energize the African continent, and for export.

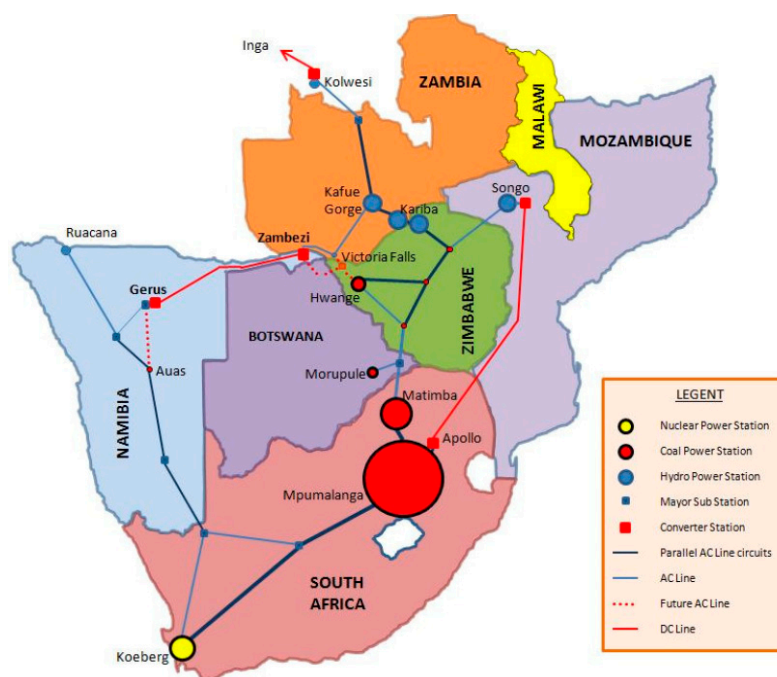


Figure 1. VSC-HVDC Caprivi Link interconnector between Namibia and Zambia [9].

The innovative application of HVDC and FACTS can contribute to power system development and resolve some operational challenges posed by demand outstripping supply, as well as environmental regulation, and address the demand for changes in the way electricity is delivered [10]. The majority of transmission lines in an electrical power transmission system are 3- ϕ AC transmission lines with changeable transmission voltages [11]. Transmission voltages continue to rise in response to a greater demand for power transmission capacity and/or longer transmission distances. Higher transmission voltages are directly associated with a reduction in technical losses [12].

HVAC transmission lines are primarily constrained by their tendency to generate large amounts of reactive power [13]. In long-distance HVAC transmission systems, the system voltage varies continuously with load changes [14]. The reactive power also varies as the load changes, which affects the system voltage. Therefore, it is essential to carry

out power system studies to determine the system parameters and their variation under different load conditions [15]. Due to the significance of power exchange, the necessity for power interconnections is expanding [16]. Utilizing HVDC schemes over long distances has various technological advantages over HVAC [17]. Advanced solutions such as HVDC and FACTS have the ability to deal with the modifications required for grid access [10].

Power pools and interconnections were built to enhance network efficiency across increasingly vast distances [18]. The power interconnection enables the export of electricity to other countries [19]. In this study, the Static Var Compensator was utilized as a part of the FACTS devices to control the system voltage by regulating reactive power [20], and the HVDC-LCC scheme was employed for the long transmission line; the results were compared with the HVAC base system. The advantages and characteristics of HVDC-LCC are available in [21]. By compensating, reactive power can be managed to enhance the performance of the AC power system [22,23]. Using DigSILENT PowerFactory, the Songo–Apollo HVDC line with an SVC (FACTS device) was modeled and a power flow study was conducted. Numerous studies demonstrate that the concurrent functioning of HVDC and FACTS devices involves interaction between control channels [24].

2. HVDC and FACTS Device Coordination

During the initial years of HVDC technology development from mercury-arc to thyristor valves, the process simultaneously reduced costs while boosting robustness [25,26]. Thus, HVDC systems and FACTS controllers based on LCC technology have a long history [27,28].

2.1. HVDC–LCC

Figure 2 shows how HVDC systems convert AC power to DC power at the rectifier terminal (sending end) and then back to AC power at the inverter terminal (receiving end) [29]. AC power is supplied to a rectifier-functioning converter. Since the rectifier outputs DC active power, it is unaffected by the frequency and phase of the AC supply [30]. Thyristor valve bridges and converter transformers comprise the thyristor-based converter topology. The conversion from alternating current to direct current is accomplished by arranging high-voltage valve bridges in a twelve- or six-pulse design, depending on the needed output voltage [29]. Due to its advantages, the HVDC–LCC line is predominantly utilized on long transmission lines transporting large amounts of power [21].

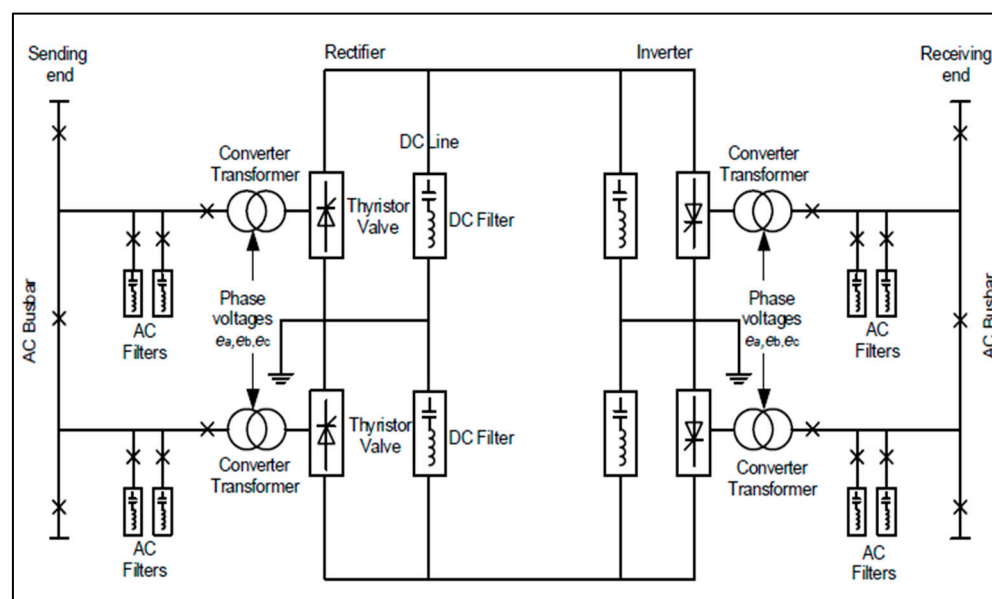


Figure 2. HVDC–LCC system.

HVDC has many advantages over HVAC [31], such as asynchronous grid connections and lower transmission losses over long distances. Therefore, the vast network is HVDC with DC cables fitted and connected with DC–DC converters. To save costs and power loss, no fast-acting DC circuit breakers (DCCBs) are utilized in the DC network [32].

2.2. Flexible AC Transmission System

FACTS devices use static equipment to transmit AC electrical power, by boosting the network's controllability and power transmission capacity; they are based on power electronics [33]. Figure 3 illustrates several types of FACTS controllers which are classified as series-connected controllers, shunt-connected controllers, combined series–shunt-connected controllers, and combined series–series-connected controllers [34]. Padiyar [1] categorized FACTS controllers depending on the power electronics equipment employed for control.

- (a) Variable impedance type comprising the Static Var Compensator (SVC)—shunt connected, Thyristor Controlled Series Capacitor (TCSC) or compensator—series-connected, and Combined Shunt and Series Thyristor Controlled Phase Shifting Transformer (TCPST) of Static PST.
- (b) Voltage Source Converter (VSC), which comprises Static Synchronous Compensator (STATCOM)—shunt coupled, Static Synchronous Series Compensator (SSSC), which is a series-connected device, Interline Power Flow Controller (IPFC)—a series–series controller, and Unified Power Flow Controller (UPFC), which is a combined shunt–series controller.

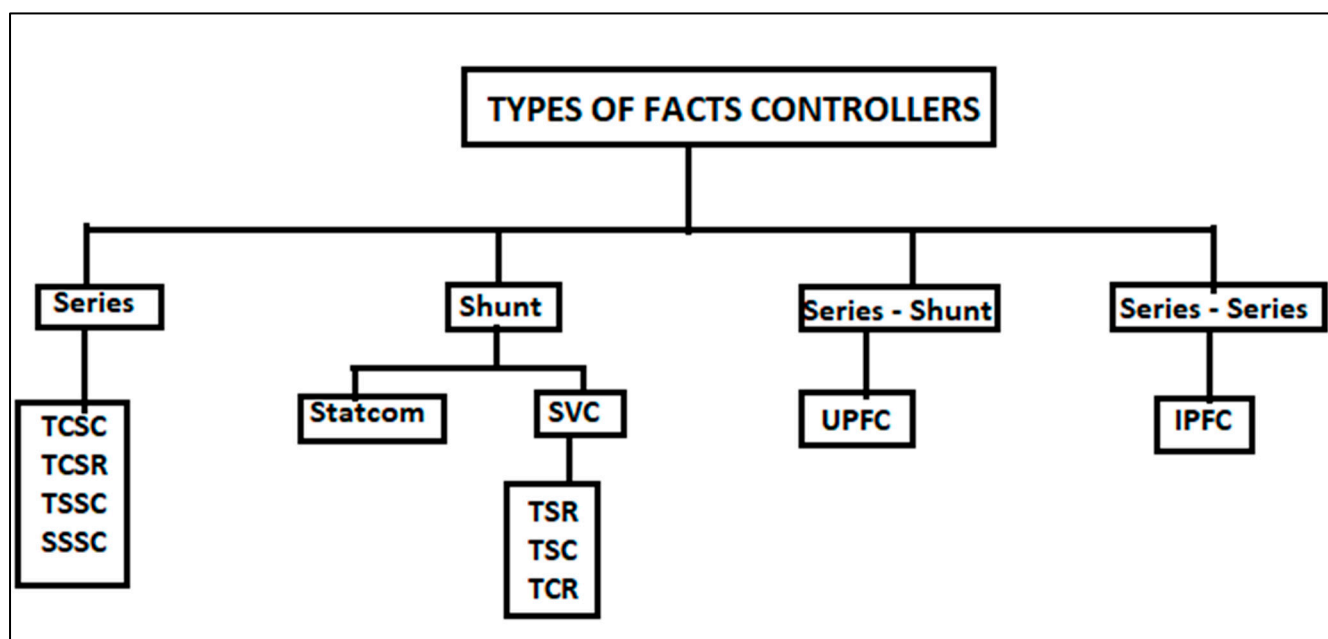


Figure 3. Four distinct forms of FACTS controllers.

Based on their switching method, the FACTS devices can be split into three groups: mechanically switched (which includes phase-shifting transformers), thyristor switched, and rapidly switched utilizing an insulated-gate bipolar transistor (IGBTs) [35]. Figure 4 illustrates the SVC family. The SVC can be used in both voltage regulation and VAR control modes [36].

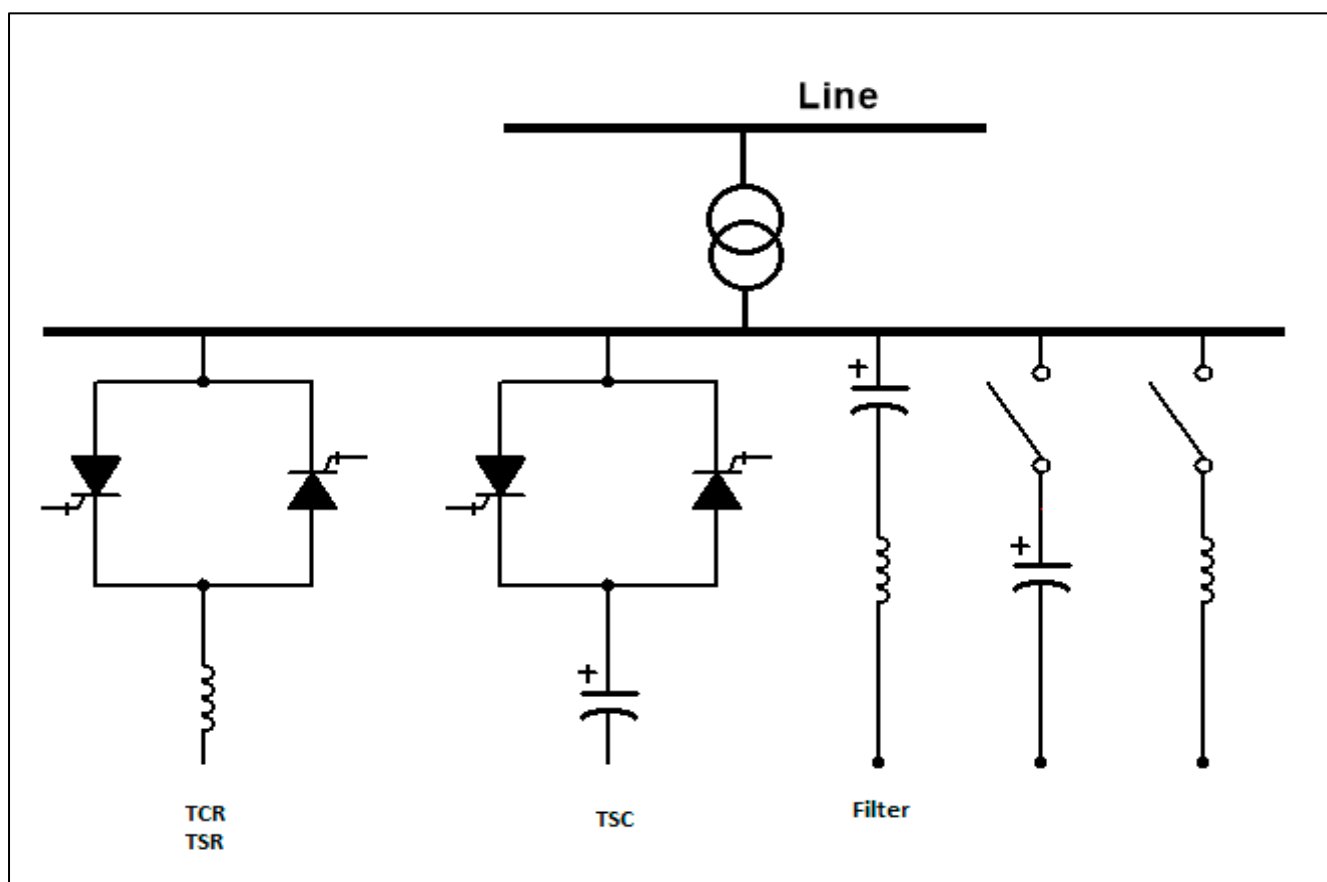


Figure 4. Static Var Compensator device.

Some forms of FACTS, such as the phase-shifting transformer (PST) and the SVC [37], are already well-known and widely employed in the power network. Recent advances in power electronics and control have expanded the application of FACTS [38]. SVCs are typically employed in power systems for voltage regulation, or as a tool to achieve system stabilization [39,40]. For adjusting the node voltage, parallel FACTS such as SVC are utilized [24]. Dr. Laszlo Gyugyi suggested UPFC as the most flexible FACTS controller for regulating voltage and power flow in a transmission line. It is made up of two voltage source converters (VSC), one shunt, and one series-connected. The two converters' DC capacitors are linked in parallel. The IPFC may be used to solve the challenge of compensating for several transmission lines at a substation. While pure series reactive (controllable) compensation (in the form of a TCSC or SSSC) can be used to control or regulate active power flow in a line, controlling reactive power is impossible unless active (actual) voltage in phase with the line current is injected [1].

2.3. Songo–Apollo HVDC–LCC Network

The Cahora Bassa HVDC inverter station is located at Apollo in South Africa [41], while the Songo Station rectifier is 1414 km north of Mozambique. The rating of the HVDC link is 1920 MW, 533 kV [42]. In 2006, Eskom awarded ABB a contract to replace eight six-pulse converters and two AC filters while preserving the existing transformers and DC sector infrastructure, incorporating the smoothing reactors [43]. Thus far, South Africa's Eskom has only one HVDC scheme between the hydroelectric power plant at the Cahora Bassa Dam in Mozambique and Johannesburg [44]. The second HVDC installation in Africa is the VSC-based Caprivi Link interconnector between Namibia and Zambia.

The 5×480 MVA generators are shown in Figure 5 as G1 to G5. Cahora Bassa is connected to the double 220 kV busbar substation in Songo, six km away [45]. Busbars are

assigned to the primary AC and DC loads. The HVDC bus is referred to as the “DC bus” while the Bindura AC line that supplies Zimbabwe is typically linked to the “AC bus” [46]. Figure 5 shows the ZESA and Eskom electricity public utilities for Zimbabwe and South Africa, respectively.

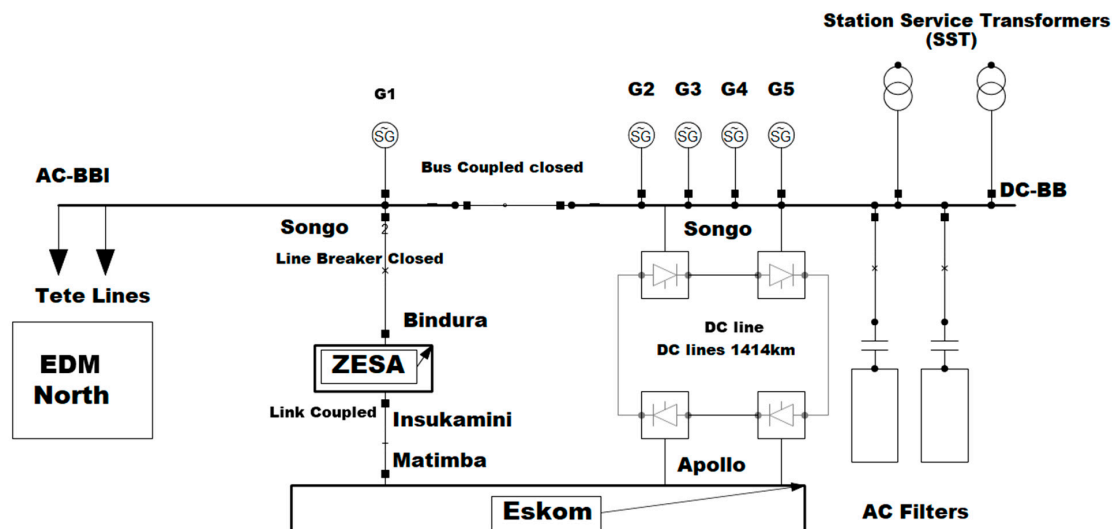


Figure 5. Static Var Compensator device single-line diagram illustrating the connection between Songo in Mozambique and Apollo in South Africa.

The hydroelectric power station at Cahora Bassa (CB) is 6 km from the Songo rectifier station. It was designed to transfer 1920 MW from the generated 2075 MW to the South African Apollo inverter station [47]. The Songo–Apollo HVDC–LCC link is shown in Figure 6. It is located in South Africa, but the rectifier is 1414 km to the north in Mozambique. The present HVDC transmission line rating is 1920 MW with 533 kV [48].

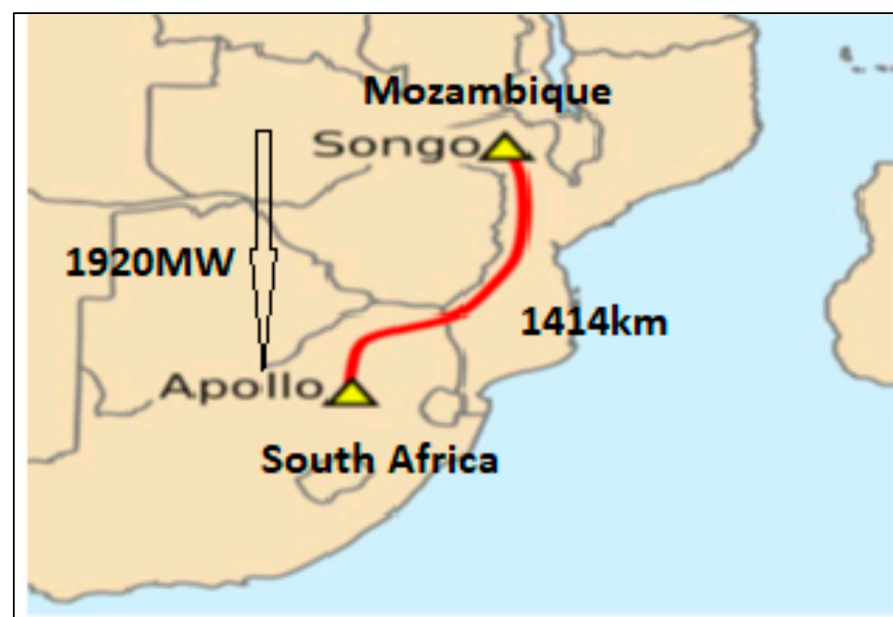


Figure 6. Songo–Apollo HVDC link.

3. Design, Modeling, Results, and Discussion of the Songo–Apollo HVDC–LCC Line

In designing and simulating the Songo–Apollo link network model, DIgSILENT PowerFactory software was utilized. The model was constructed using previously acquired

data for the Songo–Apollo transmission line. To assure the system’s reliability, an HVAC and HVDC load flow study was performed utilizing Newton Raphson’s method.

As indicated in Figure 7, the Songo–Apollo HVDC link has multiple voltage levels, with 5×480 MVA generators at Cahora Bassa rated at 220 kV. The 220–400 kV step-up transformer is used to increase the voltage to 400 kV for the 1414 km Songo–Apollo transmission line. The 275–400 kV step-down transformer is used at Apollo to reduce voltage.

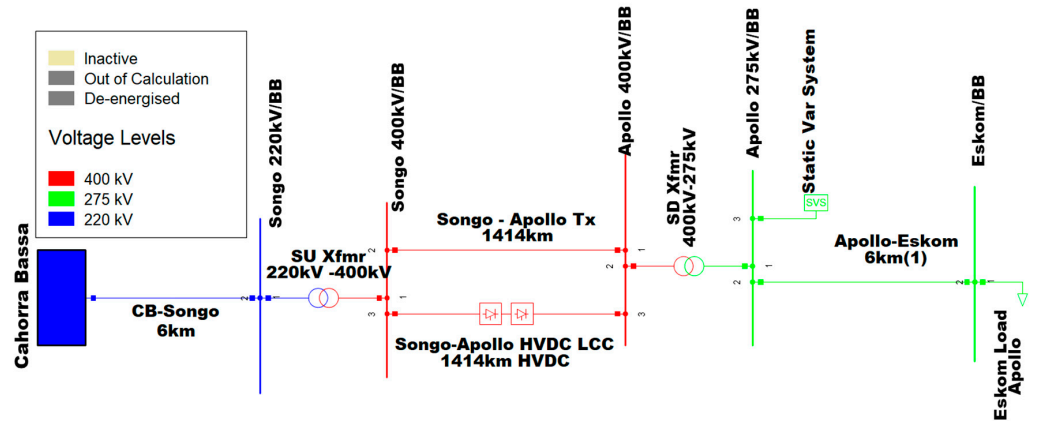


Figure 7. Songo–Apollo transmission network model.

The voltage at every busbar must be maintained within a 5% tolerance of its nominal value. In emergencies involving a failed element, the temperature rating of any equipment must not be exceeded, and the voltage must be maintained between 95% and 105% of its nominal value. However, a 15% overvoltage is permissible for five seconds, while a 20% overvoltage is acceptable for one and two seconds. Consequently, transformers, generators, and line loads must fall within the range of 80–100%, and all busbar voltages must be maintained within a tolerance of 5% of their nominal value. Figure 8 shows the Cahora Bassa generators running at full capacity, as well as the 6 km CB–Songo transmission lines. The Cahora Bassa substation is operating at 220 kV voltage (1 p.u.) as shown in Figure 8.

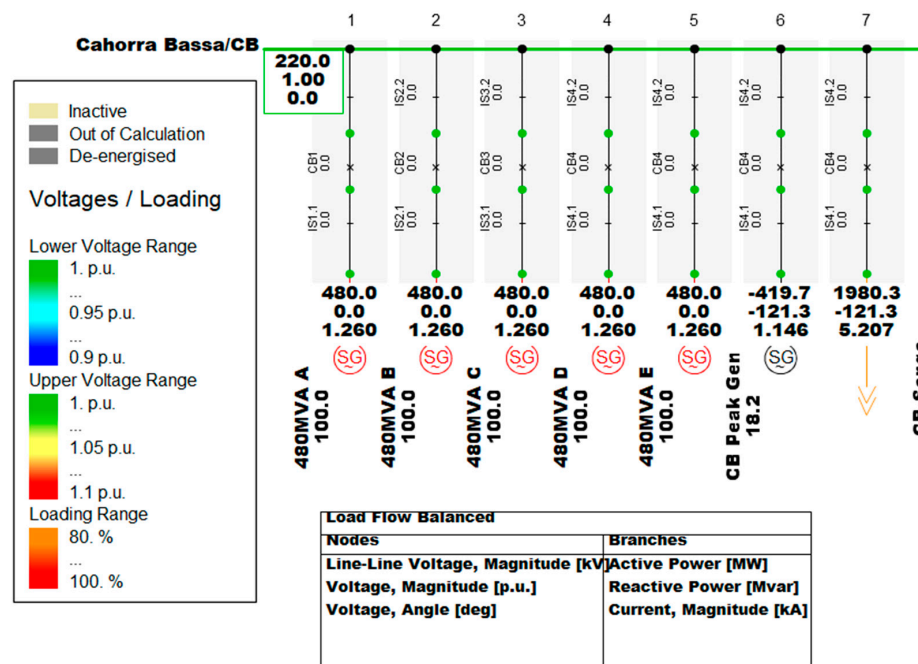


Figure 8. The 480 MVA \times 5 Cahora Bassa generator.

3.1. Songo–Apollo Transmission Line

Figure 9 shows the Songo–Apollo HVAC transmission line without the HVDC link, allowing Apollo to receive 1920 MW while producing 2003.2 MW at Cahorra Bassa. This equates to an 84.32 MW loss in the line. Voltage instability is also evident in the Apollo 400 kV bus, Apollo 275 kV bus, and Eskom bus. (See Appendix A). Cahorra Bassa exports 2004.3 MW active power, 194.4 Mvar reactive power, and 5.285 kA current flow, as shown in Figure 9.

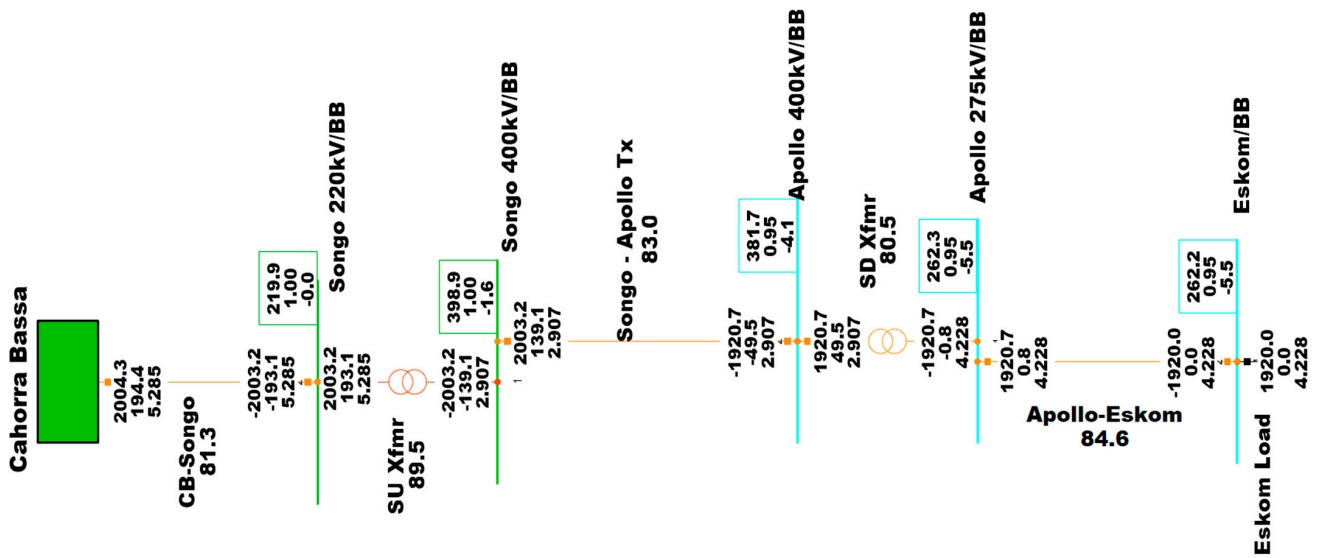


Figure 9. Songo–Apollo HVAC transmission line.

3.2. Songo–Apollo HVDC Link

Figure 10 shows the Songo–Apollo HVDC link, which is parallel to the HVAC 1414 km transmission line. The goal of the HVDC link is to minimize line losses. For the Eskom load to receive 1920 MW, Cahorra Bassa produces 1983.1 MW. The losses in the line are determined to be 63.08 MW. Consequently, losses are reduced by 21.24 MW when compared with Figure 9; thus, the voltage instability is slightly reduced (see Appendix B).

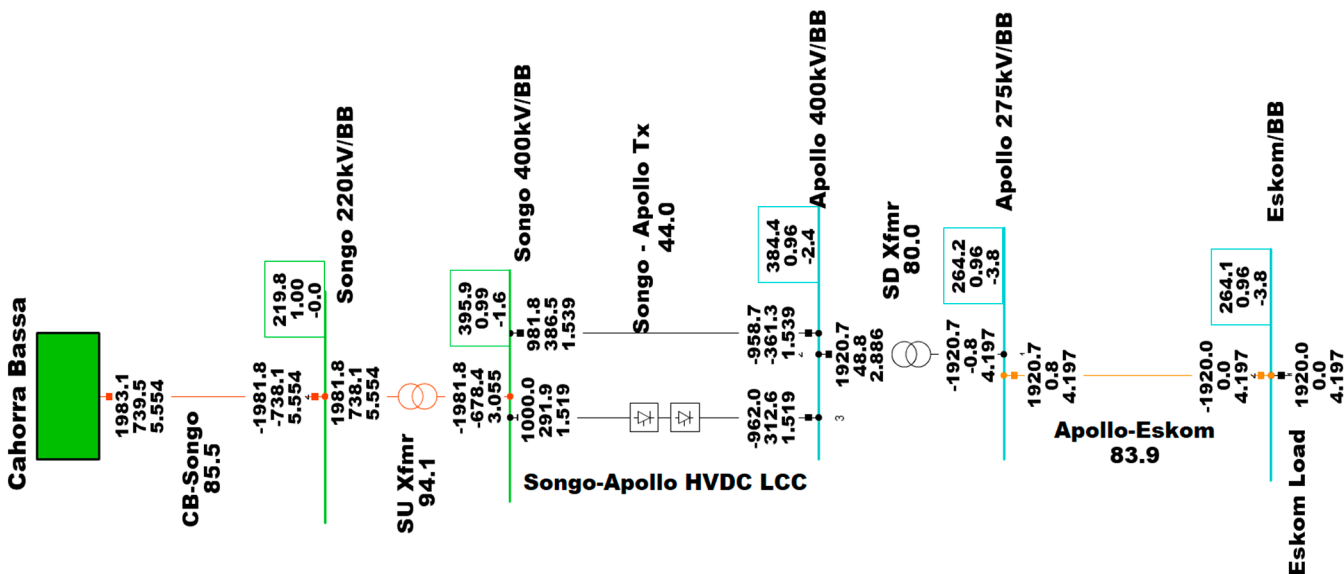


Figure 10. Songo–Apollo HVAC with HVDC link.

The DC current for an HVDC–LCC link is as follows:

$$I_{dc} = \frac{V_{dc} \cos \alpha - V_{dc} \cos \delta}{R_l + R_r + R_i} \tag{1}$$

where V_{ac} is the AC voltage, V_{dc} is the DC voltage, I_{dc} is the dc current, α is the firing angle, δ is the extinction delay angles, R_l is the resistor from the loop, R_r is the resistor from the rectifier, and R_i is the resistor from the inverter

The voltage current is:

$$V_{dc} = \frac{3\sqrt{2}}{\pi} V_{ac} \tag{2}$$

3.3. Songo–Apollo HVDC Link with SVC

Figure 11 shows the Songo–Apollo HVDC link with SVC, which is utilized to control the system’s voltage stability. To produce a 1920 MW Eskom load from the Apollo busbar, 1980.3 MW is required, which means 60.32 MW is system technical losses. It is observed that all the voltages are now between 0.99 p.u and 1.00 p.u, indicating that the SVC did regulate the voltages by managing a portion of the reactive power, given that all the voltages are now between 0.99 p.u and 1.00 p.u. The power losses for the Songo–Apollo transmission line when it was operating as an HVAC transmission line, when the HVdc link was connected along the HVAC line, and when the SVC was utilized to enhance the voltage are shown in Table 1.

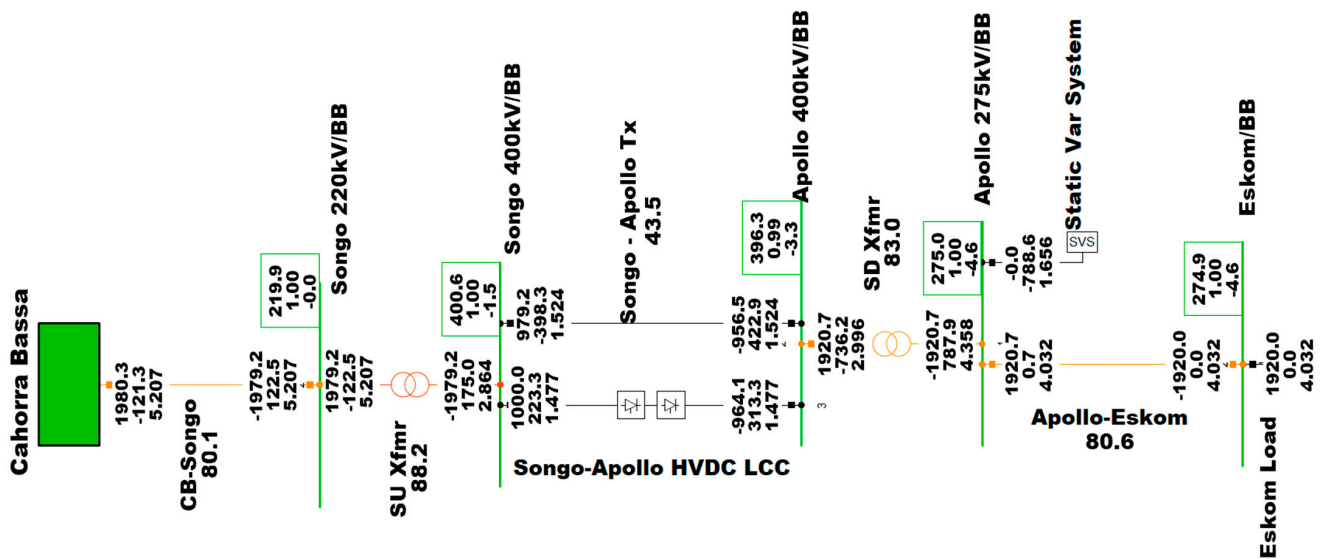


Figure 11. Songo–Apollo HVDC link with SVC.

Table 1. Each model’s power loss.

Name	Power Loss (MW)
Songo–Apollo HVAC Load Flow	84.32 MW
Songo–Apollo HVDC Link	63.08 MW
Songo–Apollo HVDC Link with SVC	60.34 MW

The SVC is then applied to the Apollo busbar to inject reactive power and regulate the voltage, as shown in Figure 10. The system represented in Figure 11 shows the Songo–Apollo link with minimum losses and enhanced voltage stability (see Appendix C).

Table 2 of the Songo–Apollo busbar shows the voltage profile for various scenarios: (a) displays the HVAC transmission line busbar voltage profile, (b) represents the busbar voltage profile for Songo–Apollo when HVDC–LCC is used to reduce long-distance losses, and (c) displays the busbar voltage for a model consisting of an HVDC–LCC link and an

SVC. The results were generated by DIGSILENT PowerFactory based on the performance of the Songo–Apollo network under various conditions. According to Table 2 below, the use of the SVC in the Apollo 275 kV busbar improves voltage stability because all voltages connected to the busbar with the SVC increased to approximately 1 p.u.

Table 2. Different busbar voltage profiles for the Songo–Apollo network.

Busbar Name	(a) HVAC (p.u)	(b) HVDC Link (p.u)	(c) HVDC and SVC (p.u)
Songo 220 kV	0.999	0.999	0.999
Songo 400 kV	0.997	0.989	1.001
Apollo 400 kV	0.954	0.961	0.991
Apollo 275 kV	0.954	0.960	1
Eskom	0.953	0.960	0.999
Cahora Bassa	1	1	1

Table 3 shows transmission line loading for several different scenarios: (a) when examining the load flow between Songo and Apollo with all HVAC lines; (b) when the load flow study was performed on Songo–Apollo HVDC–LCC connections; and (c) when a load flow study was performed on the Songo–Apollo network with LCC–HVDC and SVC in the Apollo 275 kV busbar.

Table 3. Different transmission line loading profiles for the Songo–Apollo network.

Transmission Line Name	(a) HVAC (%)	(b) HVDC Link (%)	(c) HVDC and SVC (%)
Apollo–Eskom	84.55449	83.94794	80.64736
CB–Songo	81.3024	85.45054	80.10344
Songo–Apollo Tx	83.04459	43.96473	43.5309

Table 4 shows transmission line losses under three distinct conditions: (a) when the Songo–Apollo network load flow analysis is performed on all HVAC lines; (b) when the load flow analysis is conducted using HVDC–LCC links, for which losses dropped to 63 MW; and (c) when analysis is conducted using both SVC and HVDC–LCC systems, for which there were 60.4 MW total technical losses.

Table 4. Different transmission total line loss profiles for the Songo–Apollo network.

Transmission Line Name	(a) HVAC (MW)	(b) HVDC Link (MW)	(c) HVDC and SVC (MW)
Apollo–Eskom	0.7	0.7	0.7
CB–Songo	1.1	1.3	1.1
Songo–Apollo Tx	82.6	23.1	22.7
Songo–Apollo HVDC link	-	38	35.9
Total	84.4	63.1	60.4

4. Conclusions

The primary goal of this study is to conduct load flow studies on power exchanges between countries and communities within Southern Africa, particularly those without access to electricity, with minimal losses while ensuring grid reliability. This study models the interplay between the existing and established FACTS device and HVDC (LCC) on the Songo–Apollo HVDC link.

As new generations of FACTS devices are developed and deployed for industry testing at the transmission (UPFC) and distribution level (D-FACTS) to mature technology, further studies will be conducted at those levels to ascertain their inherent impact on the technical performance of these HVDC schemes and their impact on the broader, smart distribution networks and regional power grid. These aspects were not part of the current study.

DigSILENT PowerFactory was utilized to study the transmission line performance when utilizing the HVAC transmission line to transmit 1920 MW of power from Songo to Apollo. Large distances carrying massive amounts of power resulted in 84.32 MW of line losses. The HVDC–LCC was added to the existing HVAC transmission line to reduce losses, resulting in 63.08 MW of transmission line losses. Figure 10 shows the voltage instability on the Apollo receiving side, where the Apollo 400 kV and 275 kV busbars and the Eskom busbar have 0.96 p.u.

By controlling a portion of the reactive power, 850 MVar SVC is utilized to decrease voltage instability in all busbars connected to the SVC busbar. Figure 11 represents an entire model with both HVDC–LCC and SVC, where it is determined that the transmission line losses are 60.34 MW (See Table 1). The voltage instability is controlled as seen in Figure 11, with the Apollo 400 kV busbar at 0.99 and the Apollo 275 kV and Eskom busbars at 1 p.u. In Figure 11, losses are minimized, and voltage instability is under control, making the network more resilient.

Tables 2–4 show the respective voltage busbar profile, the transmission line loading profile, and the transmission line losses that occur in the system to compare the results of the three distinct networks that are shown in Figures 9–11. This study can be applied in the future, including the most recent FACTS controllers, such as the UPFC, which is the most adaptable FACTS controller for regulating voltage and power flow in a transmission line, with the addition of IPFC to address the issue of compensating for multiple transmission lines connected at a substation.

HVDC links and FACTS controllers have been utilized as innovative methods for increasing the entire power system performance. Through this study, it is noted that HVDC and FACTS devices offer a superior solution for the long-distance transmission of bulk power; that they improve grid resilience against unforeseen events; that the voltage is regulated and the power is optimized through the HVDC–LCC and SVC systems; and that HVDC–LCC and SVC are used to control and optimize voltage and power, respectively. With further interconnections planned across Africa, this study provides preliminary insight into how large power networks with several power interconnections will enhance electricity trading and power exchanges throughout the African region or among African power pools.

Author Contributions: Conceptualization, N.W.N. and I.E.D.; methodology, N.W.N. and I.E.D.; software and validation, N.W.N. and I.E.D.; formal analysis, N.W.N.; investigation, N.W.N.; resources, I.E.D.; data curation, N.W.N. and I.E.D.; writing—original draft preparation, N.W.N.; writing—review and editing, I.E.D.; supervision, I.E.D.; project administration, I.E.D.; funding acquisition, I.E.D. All authors have read and agreed to the published version of the manuscript.

Funding: This research study received no external funding, and the APC was funded by the Smart Grids Research Centre and the Faculty Research Coordination, Faculty of Engineering and the Built Environment, Durban University of Technology, Durban, South Africa.

Acknowledgments: The authors acknowledge the facility support from the Durban University of Technology Smart Grid Research Center.

Conflicts of Interest: The authors declare no conflict of interest.

Appendix A

Load Flow Calculation				Grid Summary	
AC Load Flow, balanced, positive sequence				Automatic Model Adaptation for Convergence	No
Automatic tap adjustment of transformers	No			Max. Acceptable Load Flow Error	
Consider reactive power limits	No			Bus Equations (HV)	1.00 kVA
				Model Equations	0.10 %
Grid: lcc hvdc	System Stage: lcc hvdc	Study Case: Study Case(1)	Annex:	/ 1	
Grid: lcc hvdc Summary					
No. of Substations	6	No. of Busbars	6	No. of Terminals	81
No. of 2-w Trfs.	2	No. of 3-w Trfs.	0	No. of syn. Machines	6
No. of Loads	1	No. of Shunts/Filters	0	No. of SVS	0
Generation	= 2004.32 MW		194.38 Mvar	2013.72 MVA	
External Infeed	= 0.00 MW		0.00 Mvar	0.00 MVA	
Inter Grid Flow	= 0.00 MW		0.00 Mvar		
Load P(U)	= 1920.00 MW		0.00 Mvar	1920.00 MVA	
Load P(Un)	= 1920.00 MW		0.00 Mvar	1920.00 MVA	
Load P(Un-U)	= 0.00 MW		0.00 Mvar		
Motor Load	= 0.00 MW		0.00 Mvar	0.00 MVA	
Grid Losses	= 84.32 MW		194.38 Mvar		
Line Charging	=		0.00 Mvar		
Compensation ind.	=		0.00 Mvar		
Compensation cap.	=		0.00 Mvar		
Installed Capacity	= 3840.00 MW				
Spinning Reserve	= 1835.68 MW				
Total Power Factor:					
Generation	= 1.00 [-]				
Load/Motor	= 1.00 / 0.00 [-]				

Figure A1. Songo–Apollo model base case summary for HVAC load flow analysis, displaying system losses, and the number of all pieces of network equipment, such as busbars, transformers, loads, and generators.

Appendix B

Load Flow Calculation				Grid Summary	
AC Load Flow, balanced, positive sequence				Automatic Model Adaptation for Convergence	No
Automatic tap adjustment of transformers	No			Max. Acceptable Load Flow Error	
Consider reactive power limits	No			Bus Equations (HV)	1.00 kVA
				Model Equations	0.10 %
Grid: lcc hvdc	System Stage: lcc hvdc	Study Case: Study Case(1)	Annex:	/ 1	
Grid: lcc hvdc Summary					
No. of Substations	6	No. of Busbars	6	No. of Terminals	81
No. of 2-w Trfs.	2	No. of 3-w Trfs.	0	No. of syn. Machines	6
No. of Loads	1	No. of Shunts/Filters	0	No. of SVS	0
Generation	= 1983.08 MW		739.49 Mvar	2116.47 MVA	
External Infeed	= 0.00 MW		0.00 Mvar	0.00 MVA	
Inter Grid Flow	= 0.00 MW		0.00 Mvar		
Load P(U)	= 1920.00 MW		0.00 Mvar	1920.00 MVA	
Load P(Un)	= 1920.00 MW		0.00 Mvar	1920.00 MVA	
Load P(Un-U)	= -0.00 MW		0.00 Mvar		
Motor Load	= 0.00 MW		0.00 Mvar	0.00 MVA	
Grid Losses	= 63.08 MW		134.98 Mvar		
Line Charging	=		0.00 Mvar		
Compensation ind.	=		0.00 Mvar		
Compensation cap.	=		0.00 Mvar		
Installed Capacity	= 3840.00 MW				
Spinning Reserve	= 1856.92 MW				
Total Power Factor:					
Generation	= 0.94 [-]				
Load/Motor	= 1.00 / 0.00 [-]				

Figure A2. Songo–Apollo network model with base case summary of HVAC with HVDC connection load flow analysis illustrating the losses incurred in the line with the influence of the LCC–HVDC link.

Appendix C

Load Flow Calculation				Grid Summary	
AC Load Flow, balanced, positive sequence		Automatic Model Adaptation for Convergence	No		
Automatic tap adjustment of transformers	No	Max. Acceptable Load Flow Error			
Consider reactive power limits	No	Bus Equations(HV)		1.00 kVA	
		Model Equations		0.10 \$	
Grid: lcc hvdc	System Stage: lcc hvdc	Study Case: Study Case(1)	Annex:	/ 1	
Grid: lcc hvdc	Summary				
No. of Substations	6	No. of Busbars	6	No. of Terminals	81
No. of 2-w Trfs.	2	No. of 3-w Trfs.	0	No. of syn. Machines	6
No. of Loads	1	No. of Shunts/Filters	0	No. of asyn.Machines	0
No. of SVS					1
Generation	= 1980.32 MW	-121.29 Mvar		1984.03 MVA	
External Infeed	= 0.00 MW	0.00 Mvar		0.00 MVA	
Inter Grid Flow	= 0.00 MW	0.00 Mvar			
Load P(U)	= 1920.00 MW	0.00 Mvar		1920.00 MVA	
Load P(Un)	= 1920.00 MW	0.00 Mvar		1920.00 MVA	
Load P(Un-U)	= 0.00 MW	0.00 Mvar			
Motor Load	= 0.00 MW	0.00 Mvar		0.00 MVA	
Grid Losses	= 60.32 MW	130.77 Mvar			
Line Charging	=	0.00 Mvar			
Compensation ind.	=	0.00 Mvar			
Compensation cap.	=	-788.64 Mvar			
Installed Capacity	= 3840.00 MW				
Spinning Reserve	= 1859.68 MW				
Total Power Factor:					
Generation	= 1.00 [-]				
Load/Motor	= 1.00 / 0.00 [-]				

Figure A3. Songo–Apollo network base case overview of the HVAC load flow analysis with both LCC–HVDC connection and Static Var System, demonstrating significantly reduced losses and enhanced voltage stability, which improve the reliability of the grid.

References

1. Padiyar, K.R. *FACTS Controllers in Power Transmission and Distribution*; New Age International Publishers: New Delhi, India, 2007.
2. Hingorani, N.G. Power electronics in electric utilities: Role of power electronics in future power systems. *Proc. IEEE* **1988**, *76*, 481–482. [CrossRef]
3. Busch, S.; de Felice, M.; González, I.H. Analysis of the Water-Power Nexus in the Southern African Power Pool. European Union 2020. Available online: <https://ec.europa.eu/jrc> (accessed on 6 May 2022).
4. Justo, J.J.; Mwasilu, F.; Jung, J.-W. Doubly-fed induction generator based wind turbines: A comprehensive review of fault ride-through strategies. *Renew. Sustain. Energy Rev.* **2015**, *45*, 447–467. [CrossRef]
5. Magg, T.; Manchen, M.; Krige, E.; Wasborg, J.; Sundin, J. Connecting networks with VSC HVDC in Africa: Caprivi Link interconnector. In Proceedings of the IEEE Power and Energy Society Conference and Exposition in Africa: Intelligent Grid Integration of Renewable Energy Resources (PowerAfrica), Johannesburg, South Africa, 9–13 July 2012; pp. 1–6. [CrossRef]
6. Magg, T.; Manchen, M.; Krige, E.; Kandji, E.; Palsson, R.; Wasbor, J. Caprivi Link HVDC Interconnector: Comparison between energized system testing and real-time simulator testing. In *2012 CIGRE Session*; CIGRE: Paris, France, 2012; Volume 4, pp. 1–16.
7. Davidson, I. “Energizing Africa’s Emerging Economy—Through A Smart Integrated Electric Power Super-Grid”, DUT Inaugural Lecture Series, Durban University of Technology, Mansfield Hall, Ritson Campus, 25th October 2018. Available online: <https://www.dut.ac.za/prof-davidson-aims-to-make-africa-the-most-electrified-continent-in-the-world/> (accessed on 18 May 2022).
8. Davidson, I.E. A review of long-distance UHVDC technology-A future energy disrupter. In Proceedings of the 2020 Clemson University Power Systems Conference (PSC), Clemson, SC, USA, 10–13 March 2020; pp. 1–5. [CrossRef]
9. Kalair, A.; Abas, N.; Khan, N. Comparative study of HVAC and HVDC transmission systems. *Renew. Sustain. Energy Rev.* **2016**, *59*, 1653–1675. [CrossRef]
10. Feltes, J.; Gemmel, B.; Retzmann, D. From smart grid to super grid: Solutions with HVDC and FACTS for grid access of renewable energy sources. In Proceedings of the 2011 IEEE Power and Energy Society General Meeting, Detroit, MI, USA, 24–28 July 2011; pp. 1–6. [CrossRef]
11. Mathur, R.M.; Varma, R.K. *Thyristor-Based FACTS Controllers for Electrical Transmission Systems*; John Wiley & Sons: Hoboken, NJ, USA, 2002.

12. Liu, Z. *Ultra-High Voltage AC/DC Grids*, 1st ed.; Academic Press Elsevier: Cambridge, MA, USA, 2014.
13. May, T.W.; Yeap, Y.M.; Ukil, A. Comparative evaluation of power loss in HVAC and HVDC transmission systems. In Proceedings of the 2016 IEEE Region 10 Conference (TENCON), Singapore, 22–25 November 2016; pp. 637–641. [[CrossRef](#)]
14. Islam, A.; Al-Amin, M.; Haque, I. *Reactive Power Management at High Voltage Long AC Transmission Line*; Daffodil International University: Dhaka, Bangladesh, 2020.
15. İnci, M. Active/reactive energy control scheme for grid-connected fuel cell system with local inductive loads. *Energy* **2020**, *197*, 117191. [[CrossRef](#)]
16. Wijayatunga, P.; Chattopadhyay, D.; Fernando, P.N. Cross-Border Power Trading in South Asia: A Techno Economic Rationale. 2015. Available online: <http://hdl.handle.net/11540/5130> (accessed on 3 June 2022).
17. Alassi, A.; Bañales, S.; Ellabban, O.; Adam, G.; MacIver, C. HVDC transmission: Technology review, market trends and future outlook. *Renew. Sustain. Energy Rev.* **2019**, *112*, 530–554. [[CrossRef](#)]
18. Maupin, A. *Building a Regional Electricity Market: SAPP Challenges*; European Centre for Development Policy Management: Maastricht, The Netherlands, 2013; p. 6.
19. Kangwa, N.M.; Venugopal, C.; Davidson, I.E. A review of the performance of VSC-HVDC and MTDC systems. In Proceedings of the 2017 IEEE PES PowerAfrica, Accra, Ghana, 27–30 June 2017; pp. 267–273. [[CrossRef](#)]
20. Kincic, S.; Wan, X.; McGillis, D.; Chandra, A.; Ooi, B.-T.; Galiana, F.; Joos, G. Voltage Support by Distributed Static VAR Systems (SVS). *IEEE Trans. Power Deliv.* **2005**, *20*, 1541–1549. [[CrossRef](#)]
21. Oni, O.E.; Davidson, I.E.; Mbangula, K.N. A review of LCC-HVDC and VSC-HVDC technologies and applications. In Proceedings of the 2016 IEEE 16th International Conference on Environment and Electrical Engineering (EEEIC), Florence, Italy, 7–10 June 2016; pp. 1–7. [[CrossRef](#)]
22. Adewuyi, O.B.; Shigenobu, R.; Ooya, K.; Senjyu, T.; Howlader, A.M. Static voltage stability improvement with battery energy storage considering optimal control of active and reactive power injection. *Electr. Power Syst. Res.* **2019**, *172*, 303–312. [[CrossRef](#)]
23. Lee, Y.; Song, H. A Reactive Power Compensation Strategy for Voltage Stability Challenges in the Korean Power System with Dynamic Loads. *Sustainability* **2019**, *11*, 326. [[CrossRef](#)]
24. Xu, L.; Dong, P.; Liu, M. A comparative analysis of the interaction between different FACTS and HVDC. In Proceedings of the 2012 IEEE Power and Energy Society General Meeting, San Diego, CA, USA, 22–26 July 2012; pp. 1–5. [[CrossRef](#)]
25. Joseph, T.; Ugalde-Loo, C.E.; Liang, J.; Coventry, P.F. Asset Management Strategies for Power Electronic Converters in Transmission Networks: Application to HvdC and FACTS Devices. *IEEE Access* **2018**, *6*, 21084–21102. [[CrossRef](#)]
26. Lei, X.; Braun, W.; Buchholz, B.; Povh, D.; Retzmann, D.; Teltsch, E. Coordinated operation of HVDC and FACTS. In Proceedings of the PowerCon 2000. 2000 International Conference on Power System Technology. Proceedings (Cat. No. 00EX409), Perth, WA, Australia, 4–7 December 2000; Volume 1, pp. 529–534. [[CrossRef](#)]
27. Gemmill, B.; Dorn, J.; Retzmann, D.; Soerangr, D. Prospects of multilevel VSC technologies for power transmission. In Proceedings of the 2008 IEEE/PES Transmission and Distribution Conference and Exposition, Chicago, IL, USA, 21–24 April 2008; pp. 1–16. [[CrossRef](#)]
28. BAndersen, R. Cigre and trends in power electronics for the grid. In Proceedings of the 2013 15th European Conference on Power Electronics and Applications (EPE), Lille, France, 2–6 September 2013; pp. 1–8. [[CrossRef](#)]
29. M’Builu-Ives, S. Stability Enhancement of HVAC Grids Using HVDC Links. Master’s Thesis, College of Agriculture, Engineering and Science, University of Kwazulu Natal, Durban, South Africa, 2016.
30. Zhang, F.; Xin, H.; Wu, D.; Wang, Z.; Gan, D. Assessing Strength of Multi-Infed LCC-HVDC Systems Using Generalized Short-Circuit Ratio. *IEEE Trans. Power Syst.* **2018**, *34*, 467–480. [[CrossRef](#)]
31. Saksvik, O. HVDC technology and smart grid. In Proceedings of the 9th IET International Conference on Advances in Power System Control, Operation and Management (APSCOM 2012), Hong Kong, China, 18–21 November 2012. [[CrossRef](#)]
32. Ndlela, N.W.; Davidson, I.E. Power Planning for a Smart Integrated African Super-Grid. In Proceedings of the 2022 30th Southern African Universities Power Engineering Conference (SAUPEC), Durban, South Africa, 25–27 January 2022; pp. 1–6. [[CrossRef](#)]
33. Buraimoh, E.; Ariyo, F.K.; Omoigui, M.; Davidson, I.E. Investigation of Combined SVC and TCSC versus IPFC in Enhancing Power System Static Security. *Int. J. Eng. Res. Afr.* **2018**, *40*, 119–135. [[CrossRef](#)]
34. Zhang, X.-P.; Rehtanz, C.; Pal, B. *Flexible AC Transmission Systems: Modelling and Control*; Springer Science & Business Media: Berlin/Heidelberg, Germany, 2012.
35. Jena, R.; Chirantan, S.; Swain, S.; Panda, P. Load flow analysis and optimal allocation of SVC in nine bus power system. In Proceedings of the 2018 Technologies for Smart-City Energy Security and Power (ICESP), Bhubaneswar, India, 28–30 March 2018; pp. 1–5. [[CrossRef](#)]
36. Gandoman, F.H.; Ahmadi, A.; Sharaf, A.M.; Siano, P.; Pou, J.; Hredzak, B.; Agelidis, V.G. Review of FACTS technologies and applications for power quality in smart grids with renewable energy systems. *Renew. Sustain. Energy Rev.* **2018**, *82*, 502–514. [[CrossRef](#)]
37. Paital, S.R.; Ray, P.K.; Mohanty, A.; Dash, S. Stability improvement in solar PV integrated power system using quasi-differential search optimized SVC controller. *Optik* **2018**, *170*, 420–430. [[CrossRef](#)]
38. Jena, R.; Swain, S.C.; Dash, R. Power flow simulation & voltage control in a SPV IEEE-5 bus system based on SVC. *Mater. Today Proc.* **2020**, *39*, 1934–1940.

39. Hammad, A.E. Analysis of Power System Stability Enhancement by Static VAR Compensators. *IEEE Trans. Power Syst.* **1986**, *1*, 222–227. [[CrossRef](#)]
40. Sabai, N.; Maung, H.N.; Win, T. Voltage control and dynamic performance of power transmission system using static var compensator. *World Acad. Sci. Eng. Technol.* **2008**, *42*, 426.
41. Naidoo, P. Investigations into the Upgrading of Transmission Lines from HVAC to HVDC. Master's Thesis, School of Electrical, Electronic and Computer Engineering, University of Kwazulu Natal, Durban, South Africa, 2007.
42. Goosen, P.; Reddy, C.; Jonsson, B.; Holmgren, T.; Saksvik, O.; Bjorklund, H. Upgrade of the Apollo HVDC converter station. In Proceedings of the CIGRÉ 6th Southern Africa Regional Conference, Cape Town, South Africa, 17–21 August 2009; pp. 1–6.
43. Bjorklund, H. *Upgrading the Control System of the Square Butte HVDC Transmission*; CIGRE: Osaka, Japan, 2007; pp. 1–7.
44. OOni, E.; Davidson, I.E. Technical performance and cost analysis of a 600 kv HVDC link on South Africa's EHV network. In Proceedings of the 2017 IEEE PES PowerAfrica, Accra, Ghana, 27–30 June 2017; pp. 88–94. [[CrossRef](#)]
45. Zimba, S.K.; Houane, M.J.; Chikova, A.M. Impact of Tropical Cyclone Idai on the Southern African Electric Power Grid. In Proceedings of the 2020 IEEE PES/IAS PowerAfrica, Nairobi, Kenya, 25–28 August 2020; pp. 1–5. [[CrossRef](#)]
46. Goosen, P.; Riedel, P.; Strauss, J. GMPC enables energy transmission over interconnected SAPP grid. *IEEE Trans. Power Deliv.* **2003**, *18*, 945–952. [[CrossRef](#)]
47. Adewolu, B.O.; Saha, A.K. Performance evaluation of FACTS placement methods for available transfer capability enhancement in a deregulated power networks. In Proceedings of the 2020 International SAUPEC/RobMech/PRASA Conference, Cape Town, South Africa, 29–31 January 2020; pp. 1–6.
48. Davidson, I.E.; Oni, O.E.; Aluko, A.; Buraimoh, E. Enhancing the Performance of Eskom's Cahora Bassa HVDC Scheme and Harmonic Distortion Minimization of LCC-HVDC Scheme Using the VSC-HVDC Link. *Energies* **2022**, *15*, 4008. [[CrossRef](#)]